Int J Clin Exp Pathol (2009) 2, 370-383
www.ijcep.com/IJCEP811007

Original Article

Comparative Analysis of Paired- and Homeodomain-specific Roles in PAX3-FKHR Oncogenesis

Youbin Zhang[1], Joel Schwartz[2] and Chiayeng Wang[1]

[1]Center for Molecular Biology of Oral Diseases and [2]Department of Oral Medicine and Diagnosis and Department of Pathology, University of Illinois at Chicago, Chicago, Illinois

Received 17 November 2008; Accepted 21 November 2008; Available online 01 December 2008

Abstract: The alveolar rhabdomyosarcoma-associated t(2;13) chromosomal translocation produces an oncogenic fusion transcription factor PAX3-FKHR that combines the N-terminal DNA binding domains (paired domain and homeodomain) of PAX3 with the C-terminal activation domain of FKHR. In the context of PAX3-FKHR, the two DNA binding domains can work either cooperatively or autonomously in regulating gene transcription. The latter is a gain-of-function unique to the fusion protein. The biological activities driven by the individual DNA binding domain remains poorly defined. In this study, we express PAX3-FKHR mutants that contain only a single functional DNA binding domain into C2C12 myoblasts, and measured the *in vitro* and *in vivo* behaviors of these cells. We show that only the homeodomain-specific PAX3-FKHR mutant recapitulates the *in vitro* transformation properties of the wild type fusion protein. However, despite the differential responses *in vitro*, both the paired domain- and the homeodomain-specific PAX3-FKHR mutants promote tumor development from myoblasts *in vivo*. Our results suggest an important role for the gain of the paired domain-and the homeodomain-transcription activities in the PAX3-FKHR malignant transformation process.
Keywords: Fusion oncoprotein, rhabdomyosarcoma, tumorigenesis, nude mice

Introduction

Rhabdomyosarcoma (RMS) is a heterogeneous group of childhood cancers of the skeletal muscle lineage. Consistent chromosomal rearrangements are frequently detected in alveolar rhabdomyosarcoma (aRMS), the most aggressive subtype of RMS. The most common rearrangement is the t(2;13) chromosomal translocation that is detected in over 80% of aRMS tumors [1, 2]. The t(2;13) translocation breaks within the introns of the *PAX3* gene on chromosome 2, a muscle developmental transcription factor and the *FKHR* gene on chromosome 13, a ubiquitously expressed cell cycle regulatory and survival transcription factor, leading to the formation of a novel *PAX3-FKHR* fusion gene [3, 4]. The resulting PAX3-FKHR fusion protein consists of the intact N-terminal PAX3 DNA binding domains (the paired domain and the homeodomain) joined with the C-terminal FKHR region that contains a truncated winged-helix DNA binding domain and the activation domain.

The oncogenic potential of the PAX3-FKHR fusion protein has been well documented through a series of ectopic PAX3-FKHR expression studies in different cell culture systems [5-9]. More recently, a conditional knock-in strategy targeting PAX3-FKHR expression in differentiated muscle cells demonstrates that PAX3-FKHR plays an essential role in aRMS tumor development in mice [10, 11]. Despite these advances, the molecular mechanisms underlying PAX3-FKHR oncogenesis remain poorly understood. *In vitro* structure-function analyses have uncovered several alterations in the transcriptional and regulatory functions in PAX3-FKHR, which could contribute to the transforming activity of the fusion protein. One, by replacing a weak PAX3 activation domain with a strong FKHR activation domain, PAX3-FKHR becomes a much more potent transcription activator than

PAX3 towards the natural target genes of PAX3 [12]. Second, PAX3-FKHR is resistant to inhibition by PAX3-interacting proteins despite retaining the ability to interact with these proteins [13-16]. Third, although sharing the same DNA binding domains with PAX3, PAX3-FKHR gains the ability to control expression of genes that are not normally regulated by PAX3 [17-19]. The altered target gene specificity of PAX3-FKHR results in part from the ability of the fusion protein to uncouple the dual DNA binding requirement for PAX3 activity. In PAX3, the two DNA binding domains, the paired (PD) and the homeodomain (HD) act cooperatively to bind to and activate a composite PD/HD response element in PAX3-specific target promoters [20-22]. Unlike PAX3, PAX3-FKHR is more promiscuous in that it can activate promoters that contain only a PD or a HD response element [23, 24].

To date, direct evidence linking the altered transcriptional specificity of the PAX3-FKHR fusion protein to oncogenesis and aRMS development has yet been proven. To establish a causal relationship between altered target gene specificity and oncogenic transformation of PAX3-FKHR, we have developed C2C12 myoblast cell lines that stably express PAX3-FKHR DNA binding domain mutant proteins and compared their effects on growth, myogenic differentiation, anchorage-independent colony formation, and tumor development in nude mice to those affected by the wild type PAX3-FKHR. Our results show that each of the PD- and HD-dependent transcriptional mechanisms contributes distinctly to the malignant phenotypes of aRMS. These results provide new mechanistic insights into how chromosome translocations give rise to human malignancy.

Materials and Methods

Materials

DNA constructs expressing wild type and DNA binding domain mutants of PAX3-FKHR, and antibody specific for PAX3-FKHR were as described [25]. Antibodies specific for cyclin A (H432), cyclin E (M20), cyclin D3 (C16), Skp2 (H435), p21 (H164), p27 (N20), Myf5 (C120), Myf6 (C19) were from Santa Cruz; MyoD (5.8A), myogenin (F5D) from Pharmingen; myosin heavy chain (F47, MF20) from Developmental Studies Hybridoma Bank, and α-tubulin (ab1) from Oncogene.

Cell Culture

C2C12 myoblast cells were maintained in growth medium (Dulbecco modified Eagle's high glucose medium DMEM containing 15% fetal bovine serum). To induce myogenic differentiation, C2C12 cells were seeded at 1 x 10^6 per 100-mm dish one day before differentiation. To initiate myogenesis, cells were rinsed thoroughly with phosphate buffered saline (PBS) before adding differentiation medium (DMEM containing 2% Horse serum). Differentiation medium was replaced daily throughout the course of experiment. Stable cell lines expressing wild type and DNA binding domain mutants of PAX3-FKHR were established using pBabe based retrovirus expression system as described [24, 25]. C2C12 cells were recovered from primary tumors or lungs of nude mice by mincing the tissue with a razor blade. The minced tissue was cultured in the presence of puromycin (2 μg/ml) for three weeks to select for puromycin-resistant C2C12 cells.

Soft Agar Colony Formation Assay

Cells were cultured in a two-layer soft agar system developed by Hambruger *et al* [26]. It consisted of a 2% Noble agar underlayer and a 0.3% Noble agar overlayer containing 1 x 10^4 cells in six-well tissue culture plates. Colonies were allowed to form for a duration of three weeks with fresh media added every three days. Colonies were visualized using an inverted light microscope from which the images were captured using the MicroFire camera and PictureFrame application (Optronics). Plates were stained with crystal violet and number of colonies containing more than three cells was recorded. A minimum of three independent experiments was quantitated.

Western Blot and Immunofluorescence Assay

For immunoblotting, RIPA (20 mM Tris-HCl, pH 8.0, 137 mM NaCl, 1% NP-40, 10% glycerol, 10 μg/ml aprotinin, leupeptin, and pepstatin, 500 μM ortho-vanadate, 1mM PMSF) protein extracts were size fractionated by SDS-PAGE, and transferred to nitrocellulose membrane for antibody hybridization using an enhanced

chemiluminescence kit (ECL, Amersham, GE). For immunofluorescence, cells were fixed by paraformaldehyde, stained with anti-MHC antibody (MF20) followed by Alexa Fluor 488-conjugated secondary antibody (Molecular Probes), and visualized using a fluorescence microscope. Images of fluorescent cells were captured using the MicroFire camera and PictureFrame application (Optronics).

In vivo Tumorigenesis

Tumor induction was performed in 4-6 week-old male athymic nude mice. A total of 2 x 10^6 C2C12 or 2 x 10^5 NIH3T3 derived cells in a volume of 0.5 ml PBS was injected subcutaneously at a single site to the lower flank of each mouse. Mock injection with the same volume of PBS without cells was performed on the upper back torso of the same animal. Tumor diameter was recorded daily upon onset of nodule formation. Mice were sacrificed when the tumor size reached 2 centimeter in diameter. At the end-point of experiments, fresh tumors were extracted and photographed. Portion of the tumor was paraffin embedded for histopathological and immunohistochemical analyses. The remaining tumor tissue was used for tumor cell recovery as described in the cell culture section.

Histopathology and Immunohistochemistry

For histopathology, a series of 30 four-micron sections of paraffin-embedded tumor samples was prepared and mounted on poly-L-lysine–coated slides. Alternative slides were stained with Hematoxylin & Eosin (H&E) or hybridized to antibodies specific for MyoD and myogenin. Slides were reviewed by a board-certified pathologist (J. Schwartz). Photographs were taken using an image capture station with a CCD Spot camera attached to a Leica Digital Microscope (DM2500). An average of 24 to 36 images was analyzed from each tumor group. Standard references for diagnostic analysis included the World Health Organization Classification of Soft Tissue Tumors and PathCONSULT: http://www.PathCONSULTddx.com

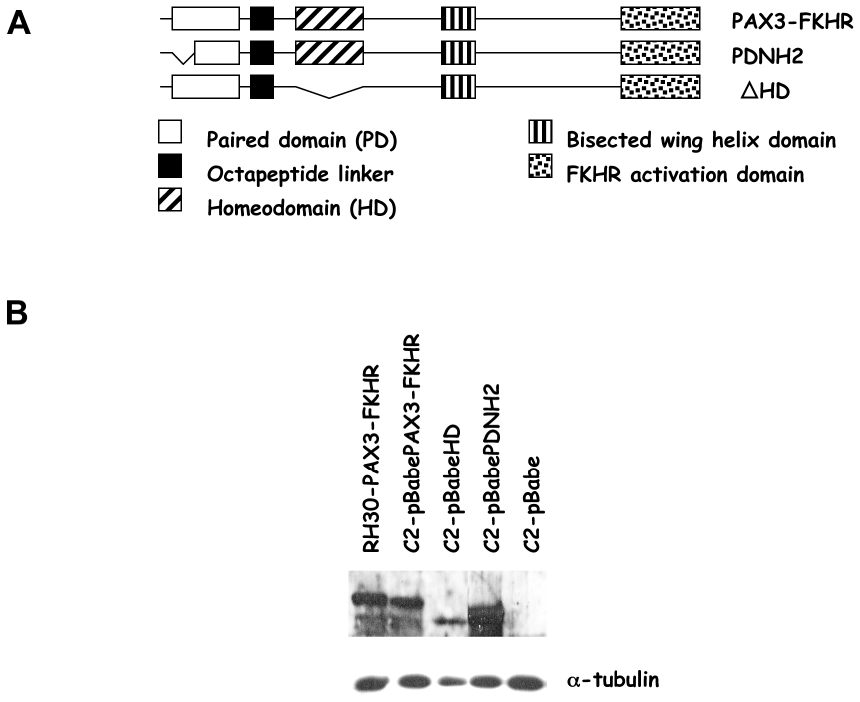

Figure 1 **A.** Schematic illustration of the wild type and DNA binding domain mutants of PAX3FKHR. **B.** Western blot analysis comparing exogenous expression of PAX3-FKHR wild type and mutant proteins in the C2C12 stable cell lines to endogenous expression of PAX3-FKHR in the RH30 aRMS cell line.

Immunohistochemical staining of the tumor sections was performed by using the Biotin-free DAB detection system and the Ventana Discovery instrument kit under conditions recommended by the manufacturers. Slides were counterstained with Hematoxylin.

Results

To test the hypothesis that the PD-dependent and HD-dependent DNA transcriptional activities were vital to PAX3-FKHR oncogenesis, we compared the *in vitro* transforming properties and *in vivo* tumorigenicity of two DNA binding domain mutants, PDNH2 (loss of PD function) or ΔHD (loss of HD function) to those of the wild type PAX3-FKHR (**Figure 1A**). Both PDNH2 and ΔHD mutants have previously been shown to be inactive towards a PAX3 (PD/HD-dependent) response element; however, they remain active towards PAX3-FKHR-specific targets that contain either a HD or PD responsive element, respectively [23, 24]. For all the experiments presented in this report, we utilized pools of retrovirally infected C2C12 myoblast cells that expressed one of the three PAX3-FKHR types (wild type, PDNH2, ΔHD) at levels similar to that of the endogenous PAX3-FKHR protein in the human aRMS RH30 cell line (**Figure 1B**). As control, we used cell pools that were infected with the empty pBabe expression vector. We will refer to the C2C12 cells expressing vector, wild type PAX3-FKHR, and DNA binding domain mutants PDNH2 and ΔHD as C2-Ba, C2-PF, C2-PDNH2, and C2-ΔHD, respectively.

Cellular Transformation Phenotypes of PAX3-FKHR Depend Critically on the HD-dependent Transcriptional Pathway in Myogenic Cells.

We began our analysis by examining what effect each of the DNA binding domain mutants had on the growth (**Figure 2**) and differentiation (**Figure 3**) of C2C12 cells in culture in comparison to the non-transformed C2-Ba and the highly transformed C2-PF cells. As in many developmental paradigms, proliferation and terminal differentiation of skeletal myoblasts are fundamentally linked. Myogenesis commences with contact inhibition of proliferating myoblasts in differentiation medium. We evaluated the growth potential by quantifying the total number of live cells under growth (GM, 15% FCS) and differentiation (DM, 2% HS) conditions (**Figure 2A**). When cells were plated under growth condition (top panel), i.e., seeded at low cell density in the presence of high serum, the C2-PDNH2 and C2-PF cells displayed a nearly identical growth curve, showing significantly increased cell number at every time point compared to the C2-ΔHD and C2-Ba cells. The C2-ΔHD and C2-Ba cells approached confluence by day six whereas the C2-PDNH2 and C2-PF cells reached confluence by day four. Although all cell types exhibited a decline in growth after day four (see inset), the C2-PDNH2 and C2-PF cells exhibited a consistently higher proliferation rate than the C2-ΔHD and C2-Ba cells at the post-confluent stage. When cells were induced to differentiate (bottom panel), i.e., seeded at high cell density in the presence of low serum, the C2-PDNH2 and C2-PF cells again had a nearly identical growth curve, showing a significantly increased cell density and growth rate than the C2-Ba cells. Interestingly, the C2-ΔHD cells displayed an intermediate growth curve, exhibiting a notably higher proliferation activity than the C2-Ba cells. This difference was first evident at day 2.

We next examined whether the C2-PDNH2 or C2-ΔHD cells could grow in an anchorage-independent manner, a key phenotypic marker for transformed cells. When grown in soft agar, the C2-PDNH2 cells proliferated rapidly and formed many large colonies within 21 days (**Figure 2B**). The efficiency of C2-PDNH2 colony formation was comparable to that of the C2-PF cells. In clear contrast, the C2-ΔHD cells behaved like the control C2-Ba cells, failing to form colonies in soft agar.

Lastly, we compared morphology (**Figure 3A**) and molecular marker expression (**Figure 3B**) following myogenic differentiation of the four cell types. At day 6 of DM treatment, the C2-PDNH2 and C2-PF cells contained predominantly undifferentiated cells with an occasional appearance of elongated tube-like structures. Interestingly, although these elongated cells stained positively with the MF20 antibody for muscle-specific myosin heavy chain (MHC), they were primarily mononucleated cells instead of the multinucleated myotubes detected in the well-differentiated control C2-Ba cells (**Figure 3A**, right panel). By contrast, the C2-ΔHD cells appeared more differentiated than the

C2-PDNH2 and C2-PF cells as determined by MF20 staining. However, the size of the C2-ΔHD myotubes was notably reduced, suggesting a possible defect in myotube fusion.

These morphological changes were accompanied by changes in molecular markers associated with muscle cell proliferation and differentiation (**Figure 3B**). Following six days of differentiation, the C2-PDNH2 and C2-PF cells maintained high levels of proliferation-associated proteins (e.g., Myf5, Skp2, cyclin A), but failed to activate comparable levels of markers characteristic of multinucleated myotubes (e.g., Myf6, MHC) and of differentiation-induced growth arrest (e.g., cyclin D3, p21, p27). Even though the C2-ΔHD cells expressed reasonable levels of late myogenesis markers (e.g., Myf6 and MHC), they did not stringently repress some of the growth-associated genes (e.g., cyclin A and Skp2). This was consistent with the continued proliferative capacity of these cells in DM (**Figure 2A**, bottom panel).

Results from **Figure 3** suggest that myogenic inhibition by PAX3-FKHR is mediated primarily through the HD-dependent transcriptional mechanism. Our finding differs from a prior report by Epstein *et al* [7], which concludes that PD/HD-dependent mechanism is involved.

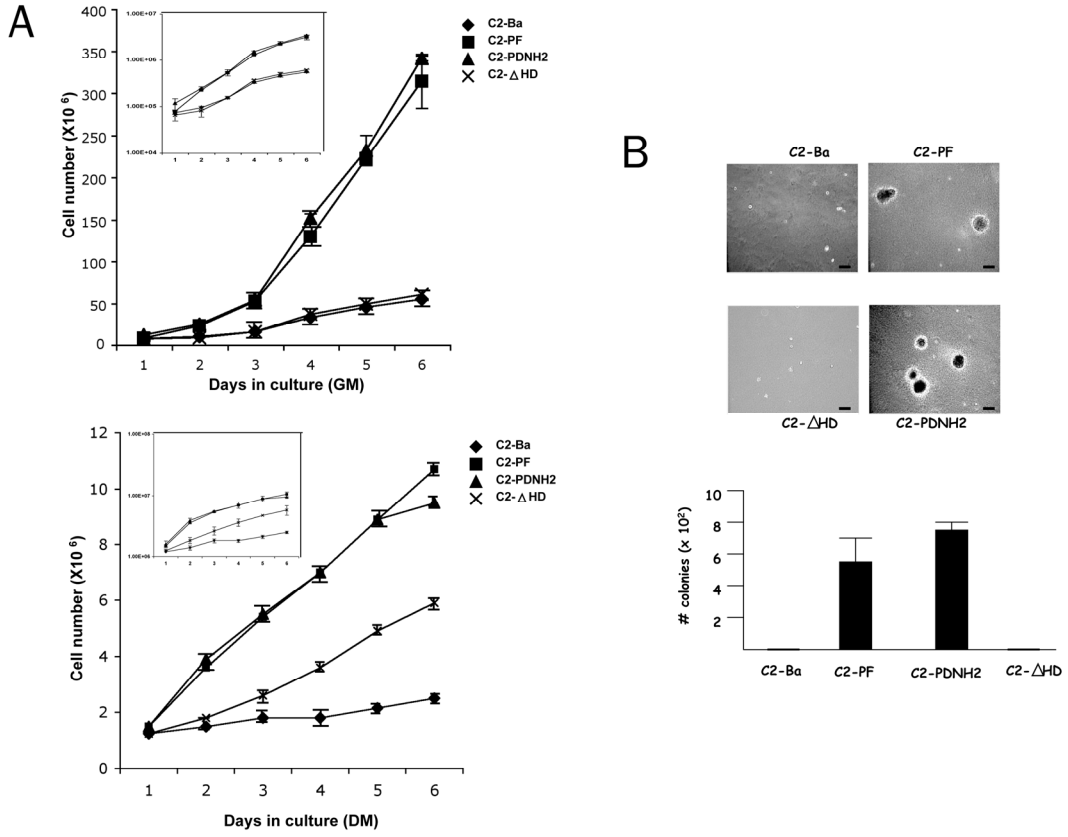

Figure 2 Effect of the wild type and DNA binding domain mutants of PAX3-FKHR on C2C12 growth patterns. **A.** Measurement of the cell numbers in C2-Ba, C2-PF, C2-PDNH2, and C2-ΔHD cultures over a six-day period under growth (GM, top panel) and differentiation (DM, bottom panel) conditions. At indicated time point, cells were harvested and stained with trypan blue. Only viable cells that excluded trypan blue were counted. The data represents an average of at least three independent experiments using different passages of pooled cells. Insets: cell number plotted on a log scale. **B.** Measurement of anchorage-independent growth of the four cell types using a colony forming soft agar assay as described in **Materials and Methods**. Scale bar: 2 μm. Top panel: light microscopic images; Bottom panel: number of colonies containing more than three cells was quantified using Image-Pro Plus software from a minimum of three independent experiments. Quantitative values represent mean ± SE.

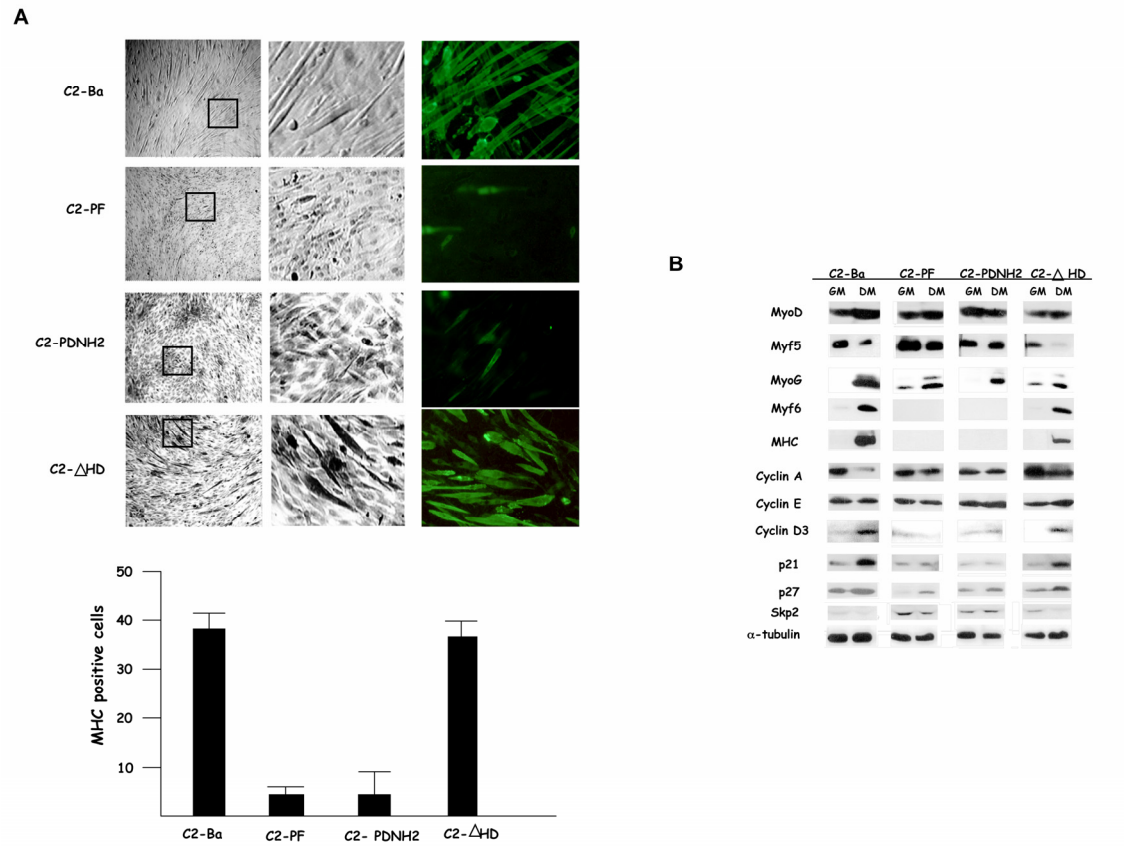

Figure 3 Effect of the wild type and DNA binding domain mutants of PAX3-FKHR on C2C12 myogenic differentiation. **A.** Top panel: light microscopic images of cells (left: 40X magnification; middle: 100X magnification of boxed regions), and fluorescent images of MF20 staining (right, 100X magnification) after six days in DM. Bottom panel: number of MF20-postiive cells was quantified from a minimum of five independent fields. Values represent mean ± SE. **B.** Western blot analysis of expression patterns of cell cycle and myogenesis specific genes under growing (GM) and six-day differentiated (DM) conditions.

Those authors examine myogenesis within colonies formed during selection of stably transfected cells. Colonies (an average of 100 cells) with a minimum of two MF20 positive cells are numerically scored as myogenesis competent. As shown in our study, we do detect a small number of MF20 positive cells in the C2-PDNH2 culture, but these MF20-positive cells do not represent the fully fused, multinucleated myotubes. Furthermore, these cells continued to proliferate well past confluence (**Figure 2B**). Thus, we believe that the apparent discrepancy stems from differences in the assays for measuring terminal myogenesis, i.e., MF20-positive vs multinucleated myotubes formation.

Growth and Morphological Differences in Primary Tumors Induced by the DNA Binding Domain Mutants of PAX3-FKHR

Tumor development *in vivo* involves a number of functions that cannot readily be modeled in cell culture. Thus, to further examine the role of PD-and HD-specific transcriptional activities in PAX3-FKHR oncogenesis, we evaluated tumor formation using a xenograft mouse model. Tumor size was recorded daily upon first detection of nodule formation. **Table 1** summarizes the average time required for the tumor to reach 1 mm or 15 mm diameter in size. The *in vivo* tumorigenic properties of the C2-PDNH2 and C2-PF cells correlated well with their *in vitro* transforming potency; mice developed tumors from both cell types at a 100% frequency with a short latency. Every mouse that was injected with the C2-PDNH2 and C2-PF cells developed 15 mm diameter tumors within 30 days, with an average of 14 (C2-PDNH2) and 20 (C2-PF) days to form a 1mm diameter tumor. Tumors developed in

Table 1 Tumorigenesis assay using xenograft athymic nude mouse model

Constructs	# Animal	# Tumor	T1	T2
C2 cells				
pBabe	12	2	60(±3)	90(±4)
PAX3-FKHR	12	12	20(±2)	30(±2)
PDNH2	6	6	14(±2)	22(±3)
ΔHD	15	15	44(±3)	75(±4)
3T3 cells				
pBabe	10	3	40(±3)	>75
PAX3-FKHR	24	24	15(±2)	24(±2)
PDNH2	16	16	12(±2)	20(±2)
ΔHD	12	4	35(±3)	>75

T1 : average days required to form 1 mm diameter tumors; T2: average days required to form 15 mm diameter tumors. In parenthesis: standard deviation as determined by Students' *t* test.

less than 10% (2 out of 12) of the control C2-Ba mice; these tumors developed very slowly, requiring an average of 60 days to reach 1 mm diameter. Surprisingly, all of the mice injected with the C2-ΔHD cells developed tumors despite the fact that these cells lacked clear transforming properties in cell culture assays. The C2-ΔHD tumors developed more slowly than the C2-PDNH2 and C2-PF tumors, requiring an average of 44 and 75 days to reach 1 mm and 15 mm tumor diameters, respectively.

We and others have previously shown that NIH3T3 fibroblast cells can be transformed by the wild type and PDNH2 mutant of PAX3-FKHR, but not by the ΔHD mutant version of the fusion protein [8, 25]. However, NIH3T3 fibroblast cells cannot undergo myogenesis, the only *in vitro* assay where we detected an altered phenotype in the C2-ΔHD cells. Thus, we performed tumorigenesis assay with the NIH3T3 cells expressing wild type and DNA binding domain mutants of PAX3-FKHR as a comparison. As expected, all mice injected with wild type PAX3-FKHR or PDNH2-expressing NIH3T3 cells developed fast growing tumors (**Table 1**). Interestingly, mice injected with the ΔHD expressing NIH3T3 cells displayed a background level of tumorigenicity similar to mice injected with the vector expressing NIH3T3 control cells. Similar observations were obtained with stable cells expressing PAX3-FKHR with different paired domain (e.g., Bu35) and homeodomain (e.g., HD-C) mutations. These results suggest that the ability of the PD-dependent pathway to induce tumors in mice is cell type-dependent.

In addition to tumor growth, there were other notable variations in the morphology and histopathology of the primary tumors. Both C2-PDNH2 and C2-PF tumors were soft, spongy, and highly vascularized with large necrotic areas; these features were largely absent in the C2-ΔHD tumors, which were solid, firm and fibrotic (**Figure 4A**). Analysis of the pathological features including cellular cohesiveness, muscle differentiation, giant cells, nuclear to cytoplasm ratio reversal, hyperchromatism, and cellular/nuclear pleomorphism suggested that the C2-PF tumors were the most aggressively transformed, followed by the C2-PDNH2 tumors, and then the C2-ΔHD tumors (**Figure 4B**). The C2-PF tumors and to a lesser extent the C2-PDNH2 tumors displayed the alveolar structure of distinct and discohesive foci separated by fibrovascular septa and small collagenous bands, which clinically distinguishes aRMS from other RMS types (**Figure 4B**, panels a/b). The alveolar structures were not noted in the C2-ΔHD tumors; these tumors were generally densely cellular and were mainly composed of a mixture of primitive rhabdomyoblasts, pericentral nucleated giant cells and spindle-shaped tumor cells associated with abundant intercellular mucoid. All three-tumor types stained positive for MyoD and myogenin (**Figure 4B**, panels c/d), two commonly used markers diagnostic for RMS tumors. Tumors from the two control mice were benign, consisting of large regions of densely packed primitive round and spindle shaped mesenchymal cells, and differentiated myofibril cells containing cross striation with a myxoid background (data not shown).

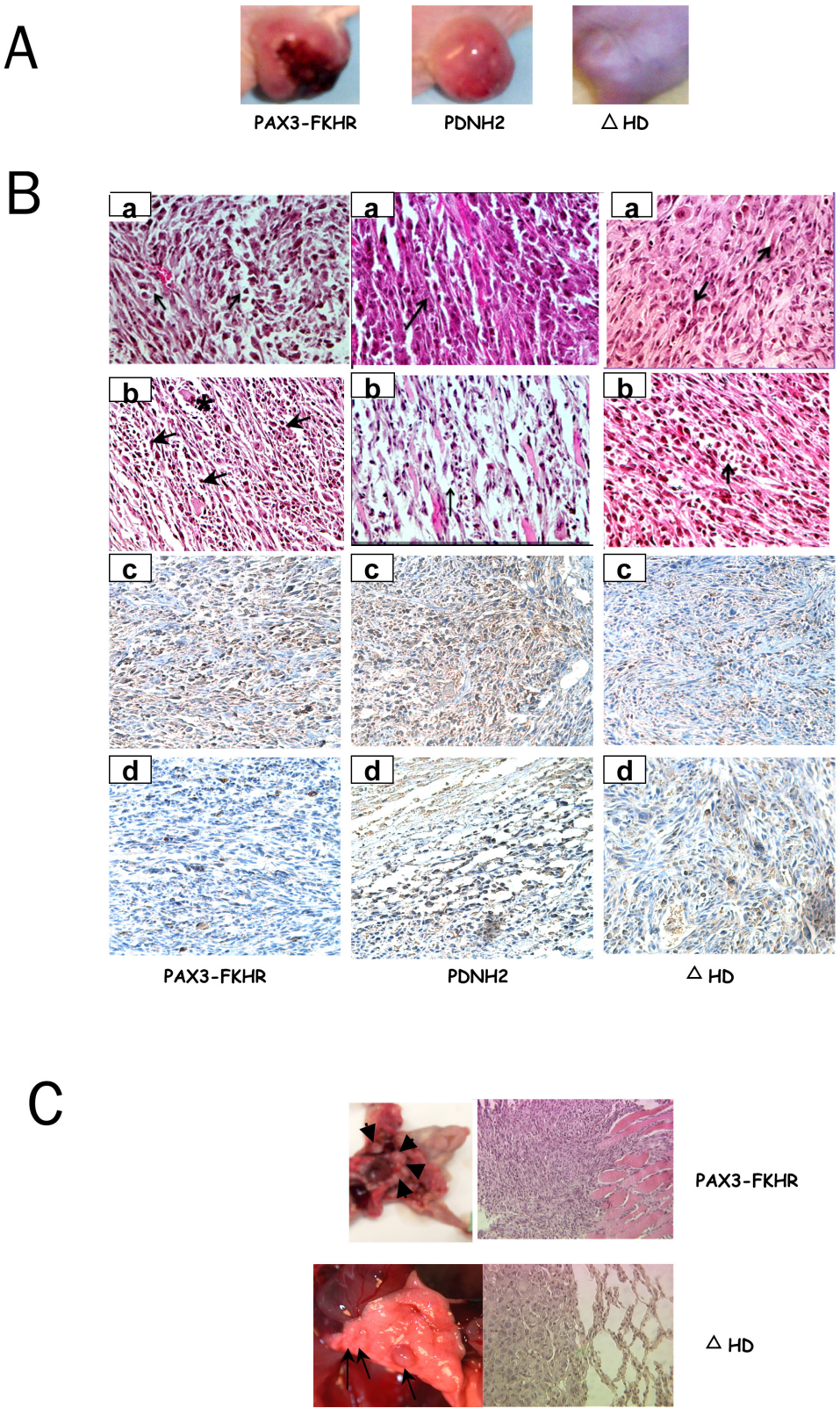

Figure 4 Histopathology and immunohistochemistry of the *in vivo* tumors formed from C2C12 cells expressing the wild type and DNA-binding domain mutants of PAX3-FKHR. **A.** Photographs of the primary tumors developed in

mice injected with the C2-PF (left), C2-PDNH2 (middle), and C2-ΔHD (right) cells. **B.** Images (200 x magnification) of representative tissue sections stained with H&E (a/b) and with antibodies specific for MyoD (c) and myogenin (d). Arrows in each image highlight the described histological features. C2-PF tumors: (a) poorly differentiated round or oval tumor cells that lose cohesion to collagenous septa; (b) increased number of tumor giant cells (*) and tumor cell aggregates separated by hyalinized fibrous septa. C2-PDNH2 tumors: (a) dense areas with cells adherent to collagenous septa forming myofibrilar bundles; (b) aggregates of discohesive round cells within nests outlined by fibrous septa and mucoid deposition. C2-ΔHD tumors: (a) predominant primitive oval cells with eccentric vesicular nuclei and spindle-shaped cells with eosinophilic cytoplasm, (b) sheets of cellular and myxoid zones. **C.** Illustration of extranodal metastasis in a mouse bearing the C2-PF tumor (top panel) and lung metastasis in a mouse bearing the C2-ΔHD tumor (bottom panel). The corresponding H&E-stained metastasized tumor sections are presented to the right of intact tissue images.

Both PD- and HD-dependent Transcriptional Mechanisms Promote Invasive Features in PAX3-FKHR Tumors.

A major factor for the poor prognosis of aRMS patients is the high degree of tumor metastasis. All three C2C12-derived PAX3-FKHR tumor types showed evidence of local invasion, suggesting that these tumors could potentially be metastatic. Visual examination at autopsy revealed secondary tumor formation in the lungs of one C2-PF and three C2-ΔHD mice (**Figure 4C**). Extra-nodal growth along the mediastinum wall was also observed in the C2-PF mouse. No tumor nodules were visible in other organs examined.

We were surprised at the seemingly higher rate of metastasis observed for the slower growing C2-ΔHD tumors. We wondered if there might not be sufficient time for secondary tumors to develop in the C2-PF and C2-PDNH2 mice because we had to sacrifice these animals within four weeks of injection due to large tumor burden. Thus, we evaluated the metastatic potential of the primary tumors by testing whether cancer cells could be detected in the lung tissue of these mice at sacrifice. To do this, we minced lung tissue and cultured cells in the presence of puromycin that would permit growth of only the C2C12 cells. Each recovered culture was verified for PAX3-FKHR and myogenic markers Myf5 and MyoD expression by Western blot analysis (data not shown). Among the mice available for examination (**Table 2**), tumor cells were recovered from the lung tissue of all of the mice injected with the C2-PF and C2-PDNH2 cells, and 80% of the mice injected with the C2-ΔHD cells. Tumor cells were not detected in the lung tissue of the control animals including the two that developed benign tumors.

We compared the anchorage-independent growth (**Figure 5A-B**) and differentiation (**Figure 5C-D**) properties of the C2C12 cells retrieved from primary tumors and from lung tissue to those of the parental cells. Results from these assays showed that both tumor and lung-derived C2-PF and C2-PDNH2 cells behaved similarly to the parental cells, i.e., they formed many large colonies in soft agar and failed to undergo terminal myogenic differentiation. Tumor and lung-derived C2-ΔHD cells displayed a more transformed phenotype than the parental cells in that they formed colonies in soft agar (**Figure 5A-B**). In addition, there was a progressive loss of myogenic differentiation potential in the recovered C2-ΔHD cells. The C2-ΔHD cells isolated from primary tumors showed a considerable reduction in the number and size of multinucleated myotubes and MF20 staining, whereas the C2-ΔHD cells derived from lung tissue completely lost the ability to differentiate (**Figure 5C-D**). The C2-Ba cells derived from the two control primary tumors behaved exactly the same as the parental cells; they remained incapable of forming colonies in soft agar, and readily differentiated into large, multinucleated myotubes.

Table 2 Frequency of tumor cell invasion into lung tissue

Constructs	# Animal tested	# Puromycin-resistant cell lines
pBabe	8	0/8(0%)
PAX3-FKHR	5	5/5(100%)
PDNH2	4	4/4(100%)
ΔHD	10	8/10(80%)*

* Of the 8 drug resistant cell lines, 5 were permanently established and three were lost to contamination.

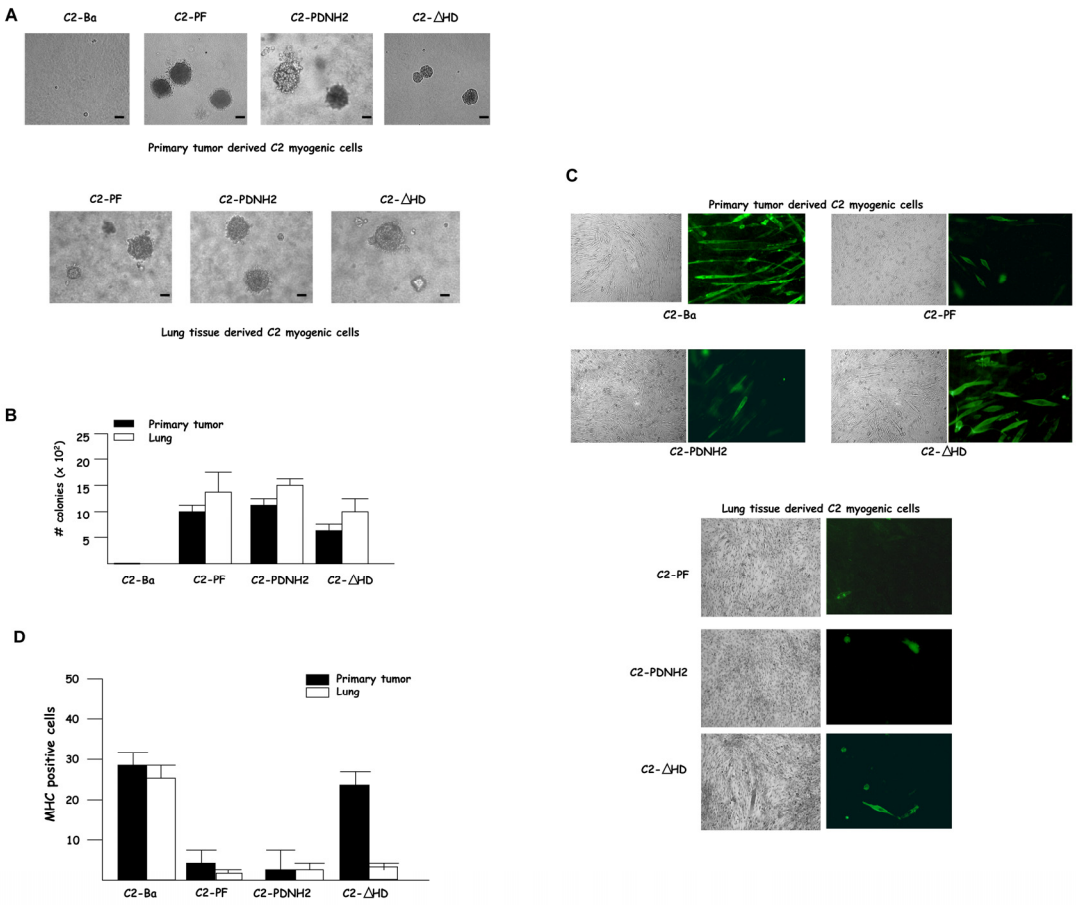

Figure 5 Evaluation of anchorage-independent growth (**A-B**) and myogenic differentiation (**C-D**) of the C2C12 cell lines recovered from primary tumors (top panels, **A** and **C**) and from lung tissue (bottom panel, **A** and **C**). Quantitative analyses of colonies (**B**) and MF20-positive cells (**D**) were as described in **Figures 2** and **3**.

Discussion

The t(2;13) chromosomal translocation occurs at a high frequency in the alveolar type of muscle tumor rhabdomyosarcoma, the most common soft tissue tumor in children and adolescents. The translocation creates a *PAX3-FKHR* fusion gene encoding a protein that is exclusively localized in the nucleus with increased transcription potency and an expanded transcriptional repertoire compared to PAX3. In this report, we have used two well-characterized DNA binding domain mutants of *PAX3-FKHR* that retain only PD-or HD-specific PAX3-FKHR transcription activity to evaluate their roles in PAX3-FKHR oncogenesis. We show for the first time that either pathway alone contributes to the oncogenic transformation of muscle cells by PAX3-FKHR.

Results from our cell culture and animal studies of the C2-PF cells attest to the functional significance of PAX3-FKHR to aRMS pathogenesis. First, PAX3-FKHR, when expressed at a level comparable to that in human aRMS tumor cells, is a highly potent transforming factor that converts C2C12 cells from an immortalized state to a tumor-like state with a diminished capacity to differentiate. Transformation by PAX3-FKHR involves complementary changes in both cell cycle and muscle regulatory factor gene expression. The selective loss of Myf6 in the C2-PF cells is particularly noteworthy because Myf6 is an obligatory myogenic regulatory factor for multinucleated myotube formation [27-29]. Since both *Myf6* and *MHC* genes are known direct downstream targets of myogenin [30-32], our results suggest that PAX3-FKHR blocks differentiation by interfering with myogenin's activation of Myf6 in C2C12 cells. This is consistent with the previous suggestion

that MyoD and myogenin proteins are functionally inactive in RMS tumor cells [33-35]. Indeed, differentiation of the C2-PF cells into multinucleated myotubes is considerably increased through ectopic expression of Myf6 (Y. Zhang and C. Wang, unpublished results).

Second, in nude mice, the highly transformed C2-PF cells form aggressive, poorly differentiated tumors that share many pathologic features with human aRMS tumor samples. In addition, all C2-PF tumor-bearing mice develop spontaneous metastasis to the lungs, one of the targeted sites for metastasis in human aRMS. The conclusions from our tumor-based study of C2-PF cells contrasts sharply to the conclusion drawn from an early report by Wang *et al* using similar cell culture and animal models [36]. In that study, the authors report less than half of the mice injected with wild type PAX3-FKHR expressing C2C12 cells developed benign and non-invasive tumors that regressed within a month. It is difficult to directly compare PAX3-FKHR protein expression levels between the two studies because the prior report only measured *PAX3-FKHR* RNA levels. However, we suspect that differences in PAX3-FKHR protein levels could be the major contributing factor to the different conclusions. The prior study uses pcDNA3 expression vector that often leads to a high level of PAX3-FKHR protein initially. We have found that PAX3-FKHR protein level from the pcDNA3 expression vector declines precipitously to near undetectable level over a few weeks in culture (our unpublished observation). This loss of expression most likely results from the reported inhibitory effect of high level PAX3-FKHR expression on cell proliferation [37]. We have overcome this problem by using retroviral vector that sustains a moderate and consistent level of PAX3-FKHR protein over several months in culture.

It is important to note that C2C12 is a spontaneously immortalized line. Thus, we cannot formally rule out the possibility that genetic mutations responsible for immortalization interact with PAX3-FKHR to produce highly aggressive and malignant phenotypes observed in our study. Indeed, secondary mutations such as in the *Ras*, *p53*, *Ink4* pathways have been reported to increase the frequency of aRMS incidence in the *PAX3-FKHR* conditional knock-in mouse model [10] and to enhance PAX3-FKHR transformation of mouse mesenchymal stem cells to form aRMS tumors in nude mice [38].

In culture, the C2-PDNH2 cells display highly transformed properties that are comparable to the morphological and molecular changes described for the C2-PF cells. Thus, it is perhaps not surprising that the C2-PDNH2 cells develop aggressive and metastatic tumors that largely resemble the C2-PF tumors *in vivo*. The overlapping *in vitro* and *in vivo* behaviors of the C2-PDNH2 and C2-PF cells allude to the pivotal role of the HD-dependent transcription pathway in PAX3-FKHR oncogenesis. The most striking finding of our study is that the C2-ΔHD cells efficiently (100%) form malignant tumors that are highly metastatic. As has been reported by others and us, HD mutants including ΔHD, have little or no effect on the proliferation and anchorage-independent growth of NIH3T3 fibroblast cells [8, 25]. Our results with the C2C12 cells measured under growth conditions are in general agreement with these prior reports. However, a more detailed analysis reveals a modest but reproducible change in the proliferation and differentiation phenotypes of C2-ΔHD cells in DM. First, we find that although the differentiated C2-ΔHD cells stain intensely for the MHC, myotube size is considerably smaller compared to that of the C2-Ba control cells, suggesting a reduced function in cell fusion. Second and perhaps more significantly, we find that the C2-ΔHD cells overcome contact inhibition and continue to proliferate for several days, long after the C2-Ba cells have ceased proliferating. We suspect that these phenotypic alterations in the C2-ΔHD cells, albeit much less drastic than the full-blown transforming phenotype observed in the C2-PDNH2 and C2-PF cells, might provide a threshold change sufficient for tumor development *in vivo*. This notion that the tumorigenic effect of the C2-ΔHD derives in part from a defect in differentiation is in line with the observation that NIH3T3 fibroblast cells, which lack an intrinsic differentiation program, are resistant to tumorigenesis by the ΔHD mutant protein (**Table 1**).

We do not think, however, that the PD-dependent mechanism alone accounts for the full-scale tumorigenesis observed. Instead, we hypothesize that the modest changes in the C2-ΔHD cells provide a permissive milieu for these cells to accumulate secondary

events that eventually result in tumor development. This could explain the lag in tumor initiation and the slower tumor growth for the C2-ΔHD cells compared to the C2-PDNH2 and C2-PF cells that are already highly transformed in culture. The C2-ΔHD cells may have acquired genetic and/or epigenetic changes in response to environmental cues present *in vivo* but missing in culture conditions. It is formally possible that tumors may have arisen from the preferential *in vivo* selection of an under-represented population of highly transformed cells from the C2-ΔHD cells. We think this is unlikely for two reasons. First, the growth and differentiation properties of the C2-ΔHD cells do not change after continuous passage in culture for several generations, when one would expect a small highly transformed population to take over the culture. Second, the C2-ΔHD cells recovered from tumors are phenotypically distinct from the parental C2-ΔHD cells; the recovered cells inherit permanent changes in their growth and differentiation properties. The C2-ΔHD cells isolated from secondary sites, such as lung tissue, are progressively more transformed than the parental C2-ΔHD cells or the C2-ΔHD cells from the primary tumor. Our results establish for the first time an independent role for the PD-dependent pathway in PAX3-FKHR tumorigenesis.

To summarize, we have provided new insights into the unique transcriptional network of PAX3-FKHR that drives myogenic cell transformation and tumorigenesis. We demonstrate for the first time that C2C12 myoblasts transformed by PAX3-FKHR form aggressive and metastatic aRMS-like tumors in nude mice. Our studies support the notion that aRMS oncogenesis arises from multiple developmental stages, including myoblastic progenitor cells in addition to mesenchymal stem cells and mature muscle as previously reported [10, 38]. Furthermore, we show that both PD-dependent and HD-dependent pathways play critical and independent, but supportive roles in the tumorigenesis. The combined action of these separate oncogenic pathways in one protein may account for the highly aggressive tumors and poor prognosis linked to fusion protein positive aRMS cases. The C2C12 model system will be amendable in future studies to help identify and characterize key players in the fusion protein regulatory pathways at various oncogenic stages, and to identify the nature of secondary event(s) associated with tumorigenesis and metastasis.

Acknowledgements

We thank Dr. Reed Graves for the critical review of this manuscript, and Dr. G. Grechko for his technical contribution in NIH3T3 cell based tumorigenic assay. The work is supported by grant from NIH (CA074907) to CW.

Please address all correspondences to Dr. Chiayeng Wang, CMBOD, University of Illinois at Chicago 801 South Paulina Street, Chicago, IL 60612. Tel: 312-996-4530; Fax: 312-413-1604; Email: chiayeng@uic.edu

References

[1] Turc-Carel C, Lizard-Nacol S, Justrabo E, Favrot M and Tabone E. Consistent chromosomal translocation in alveolar rhabdomyosarcoma. *Cancer Genet Cytogenet* 1986; 19:361-362.

[2] Wang-WS, Soukup S, Ballard E, Gotwals B and Lampkin B. Chromosomal analysis of sixteen human rhabodmyosarcomas. *Cancer Res* 1988;48:983-987.

[3] Barr FG, Galili N, Holick J, Biegel JA, Rovera G and Emanuel BS. Rearrangement of the PAX3 paired box gene in the paediatric solid tumour alveolar rhabdomyosarcoma. *Nat Genet* 1993; 3:113-117.

[4] Shapiro DN, Sublett JE, Li B, Downing JR and Naeve CW. Fusion of PAX3 to a member of the Forkhead family of transcripton factors in human alveolar rhabdomyosarcoma. *Cancer Res* 1993;53:5108-5112.

[5] Anderson J, Ramsay A, Gould S and Pritchard-Jones K. PAX3-FKHR induces morphological change and enhances cellular proliferation and invasion in rhabdomyosarcoma. *Am J Pathol* 2001;159: 1089-1096.

[6] Bernasconi M, Remppis A, Fredericks WJ, Rauscher FJ and Schafer BW. Induction of apoptosis in rhabdomyosarcoma cells through down-regulation of PAX proteins. *Proc Natl Acad Sci USA* 1996;93:13164-13169.

[7] Epstein JA, Lam P, Jepeal L, Maas RL and Shapiro DN. Pax3 inhibits myogenic differentiation of cultured myoblast cells. *J Biol Chem* 1995;270:11719-11722.

[8] Lam PY, Sublett JE, Hollenbach AD and Roussel MF. The oncogenic potential of the Pax3FKHR fusion protein requires the Pax3 homeodomain recognition helix but not the Pax3 paired-box DNA binding domain. *Mol Cell Biol* 1999;19: 594-601.

[9] Scheidler S, Fredericks WJ, Rauscher FJ, Barr FG, and Vogt PK. The hybrid PAX3-FKHR fusion

protein of alveolar rhabdomyosarcoma transforms fibroblasts in culture. *Proc Natl Acad Sci USA* 1996;93:9805-9809.
[10] Keller C, Arenkiel BR, Coffin CM, El-Bardeesy N, DePinho RA and Capecchi MR. Alveolar rhabdomyosarcomas in conditional Pax3:Fkhr mice: cooperativity of Ink4a/ARF and Trp53 loss of function. *Genes Dev* 2004;18: 2614-2626.
[11] Keller C, Hansen MS, Coffin CM and Capecchi MR. Pax3:Fkhr interferes with embryonic Pax3 and Pax7 function: implications for alveolar rhabdomyosarcoma cell of origin. *Genes Dev* 2004;18:2608-2613.
[12] Fredericks WJ, Galili N, Mukhopadhyay S, Rovera G, Bennicelli J, Barr FG and Rauscher FJ. The PAX3-FKHR fusion protein created by the t(2;13) translocation in alveolar rhabdomyosarcomas is a more potent transcriptional activator than PAX3. *Mol Cell Biol* 1995;15:1522-1535.
[13] Hollenbach AD, Sublett JE, McPherson CJ and Grosveld G. The Pax3-FKHR oncoprotein is unresponsive to the Pax3-associated repressor hDaxx. *EMBO J* 1999;18:3702-3711.
[14] Hollenbach DA, McPherson JC, Lagutina I and Grosveld G. The EF-hand calcium-binding protein calmyrin inhibits the transcriptional and DNA-binding activity of Pax3. *Biochim Biophys Acta* 2002;1574:321-328.
[15] Magnaghi P, Roberts C, Lorain S, Lipinski M and Scambler PJ. HIRA, a mammalian homologue of *Saccharomyces cerevisiae* transcriptional co-repressors, interacts with Pax3. *Nat Genet* 1998;20:74-77.
[16] Wiggan ON, Taniguchi-Sidle A and Hamel AP. Interaction of the pRB-Family proteins with factors containing paired-like homeodomains. *Oncogene* 1998;16:227-236.
[17] Begum S, Emani N, Cheung A, Wilkins O, Der S and Hamel PA. Cell-type-specific regulation of distinct sets of gene targets by Pax3 and Pax3/FKHR. *Oncogene* 2005;24:1860-1872.
[18] De Pitta C, Tombolan L, Albiero G, Sartori F, Romualdi C, Jurman G, Carli M, Furlanello C, Lanfranchi G and Rosolen A. Gene expression profiling identifies potential relevant genes in alveolar rhabdomyosarcoma pathogenesis and discriminates PAX3-FKHR positive and negative tumors. *Int J Cancer* 2006;118:2772-2781.
[19] Khan J, Bittner ML, Saal LH, Teichmann U, Azorsa DO, Gooden GC, Pavan WJ, Trent JM and Meltzer PS. cDNA microarrays detect activation of a myogenic transcription program by the PAX3-FKHR fusion oncogene. *Proc Natl Acad Sci USA* 1999;96:13264-13269.
[20] Chalepakis G, Jones FS, Eelman GM and and Gruss P. Pax-3 contains domains for transcription activation and transcription inhibition. *Proc Natl Acad Sci USA* 1994;91: 12745-12749.
[21] Chalepakis G and Gruss P. Identification of DNA recognition sequences for the Pax3 paired domain. *Gene* 1995;162:267-270.
[22] Goulding MD, Chalepakis G, Deutsch U, Erselius JR and Gruss P. Pax3, a novel murine DNA binding proein expressed during early neurogeneisis. *EMBO J* 1991;10:1135-1147.
[23] Epstein JA, Song B, Lakkis M and Wang C. Tumor-specific PAX3-FKHR transcription factor, but not PAX3, activates the platelet-derived growth factor alpha receptor. *Mol Cell Biol* 1998;18:4118-4130.
[24] Zhang L and Wang C. Identification of a new class of PAX3-FKHR target promoters: a role of the Pax3 paired box DNA binding domain. *Oncogene* 2007;26:1595-1605.
[25] Cao Y and Wang C. The COOH-terminal transactivation domain plays a key role in regulating the in vitro and in vivo function of Pax3 homeodomain. *J Biol Chem* 2000;275: 9854-9862.
[26] Hamberger AW, Salmon SE, Kim MB, Trent TM, Soehnlen B, Alberts DC and Schmidt HJ. Direct cloning of human ovarian carcinoma cells in agar. *Cancer Res* 1978;38:3438-3444.
[27] Mak KL, To RQ, Kong Y and Konieczny SF. The MRF4 activation domain is required to induce muscle-specific gene expression. *Mol Cell Biol* 1992;12:4334-4346.
[28] Vivian JL, Olson EN and Klein WH. Thoracic skeletal defects in myogenin-and MRF4-deficient mice correlate with early defects in myotome and intercostal musculature. *Dev Biol* 2000;224:29-41.
[29] Yoon JK, Olson EN, Arnold HH and Wold BJ. Different MRF4 knockout alleles differentially disrupt Myf-5 expression: cis-regulatory interactions at the MRF4/Myf-5 locus. *Dev Biol* 1997;188:349-362.
[30] Black BL, Martin JF and Olson EN. The mouse MRF4 promoter is trans-activated directly and indirectly by muscle-specific transcription factors. *J Biol Chem* 1995;270:2889-2892.
[31] Hasty P, Bradley A, Morris JH, Edmondson DG, Venuti JM, Olson EN and Klein WH. Muscle deficiency and neonatal death in mice with a targeted mutation in the myogenin gene. *Nature* 1993;364:501-506.
[32] Naidu PS, Ludolph DC, To RQ, Hinterberger TJ and Konieczny SF. Myogenin and MEF2 function synergistically to activate the MRF4 promoter during myogenesis. *Mol Cell Biol* 1995;15:2707-2718.
[33] Puri PL, Wu Z, Zhang P, Wood LD, Bhakta KS, Han J, Feramisco JR, Karin M and Wang JYJ. Induction of terminal differentiation by constitutive activation of p38 MAP kinase in human rhabdomyosarcoma cells. *Genes Dev* 2000;14:574-584.
[34] Tapscott SJ, Thayer MJ and Weintraub H. Deficiency in rhabdomyosarcomas of a factor required for MyoD activity and myogenesis. *Science* 1993;259:1450-1453.

[35] Weintraub M, Kalebic T, Helman JL and Bhatia GK. Disruption of the MyoD/p21 pathway in rhabdomyosarcoma. *Sarcoma* 1997;1:135-141.
[36] Wang W, Kumar P, Wang W, Epstein J, Helman L, Moore JV and Kumar S. Insulin-like growth factor II and PAX3-FKHR cooperate in the oncogenesis of rhabdomyosarcoma. *Cancer Res* 1998;58:4426-4433.
[37] Xia SJ and Barr FG. Analysis of the transforming and growth suppressive activities of the PAX3-FKHR oncoprotein. *Oncogene* 2004;23:6864-6871.
[38] Ren YX, Finckenstein FG, Abdueva DA, Shahbazian V, Chung B, Weinberg KI, Triche TJ, Shimada H and Anderson MJ. Mouse mesenchymal stem cells expressing PAX-FKHR form alveolar rhabdomyosarcomas by cooperating with secondary mutations. *Cancer Res* 2008;68:6587-6597.